EVALUATION AND TEST OF A CRACK INITIATION FOR A 316 SS CYLINDRICAL Y-JUNCTION STRUCTURE IN A LIQUID METAL REACTOR

CHANG-GYU PARK*, JONG-BUM KIM and JAE-HAN LEE
Korea Atomic Energy Research Institute
150 Deokjin-dong, Yuseong-gu, Daejeon, 305-353, Korea
*Corresponding author. E-mail : chgpark@kaeri.re.kr

A liquid metal reactor (LMR) operated at high temperatures is subjected to both cyclic mechanical loading and thermal loading; thus, creep-fatigue is a major concern to be addressed with regard to maintaining structural integrity. The Korea Advanced Liquid Metal Reactor (KALIMER), which has a normal operating temperature of 545°C and a total service life time of 60 years, is composed of various cylindrical structures, such as the reactor vessel and the reactor baffle. This study focuses on the creep-fatigue crack initiation for a cylindrical Y-junction structure made of 316 stainless steel (SS), which is subjected to cyclic axial tensile loading and thermal loading at a high-temperature hold time of 545°C. The evaluation of the considered creep-fatigue crack initiation was carried out utilizing the σ_d approach of the RCC-MR A16 guide, which is the high-temperature defect assessment procedure. This procedure is based on the total accumulated strain during the service time. To confirm the evaluated result, a high-temperature creep-fatigue structural test was performed. The test model had a circumferential through wall defect at the center of the model. The defect front of the test model was investigated after the 100th cycle of the testing by utilizing a metallurgical inspection technique with an optical microscope, after which the test result was compared with the evaluation result. This study shows how creep-fatigue crack initiation for a high-temperature structure can be predicted with conservatism per the RCC-MR A16 guide.

KEYWORDS : KALIMER, Creep-Fatigue, Crack Initiation, Y-junction Structure, RCC-MR A16

1. INTRODUCTION

The operating conditions of liquid metal reactor (LMR) plants generally include high temperatures of above 500°C and low pressures of below 10 bar. The low-pressure and high-temperature conditions in an LMR encourage the use of ductile materials, which decrease the risk of an unstable fracture occurrence. The LMR structures are exposed to cyclic thermal loading and mechanical loading during reactor operation. All reactor structures are designed as defect-free structures; nonetheless, a given reactor structure might contain initial defects, such as weld defects incurred during the manufacturing process or creep-fatigue defects incurred during an operating lifetime. Therefore, creep-fatigue crack initiation evaluations are necessary to ensure the integrity of reactor structures at high temperatures [1].

The Korea Atomic Energy Research Institute (KAERI) has been developing a pool-type sodium-cooled liquid metal reactor, the KALIMER-600 (Korea Advanced Liquid Metal Reactor, 600MWe), which is currently at the conceptual design stage [2]. Figure 1 shows the conceptually designed KALIMER-600 reactor structures, including the containment vessel, reactor vessel, reactor baffle, and other components.

In this study, an evaluation of the creep-fatigue crack initiation for a cylindrical Y-junction structure with a circumferential through wall defect was conducted by use of the RCC-MR[3] A16 guide[4], and a high-temperature creep-fatigue crack initiation test was carried out. The A16 guide proposes defect assessment procedures based on the fracture mechanics corresponding to a specific loading condition. A finite element (FE) stress analysis was performed to characterize the stress distribution near the defect front of a cylindrical Y-junction structure. Additionally, a creep-fatigue crack-initiation test was performed, and the crack initiation at the defect front was examined through a metallurgical inspection with an optical microscope.
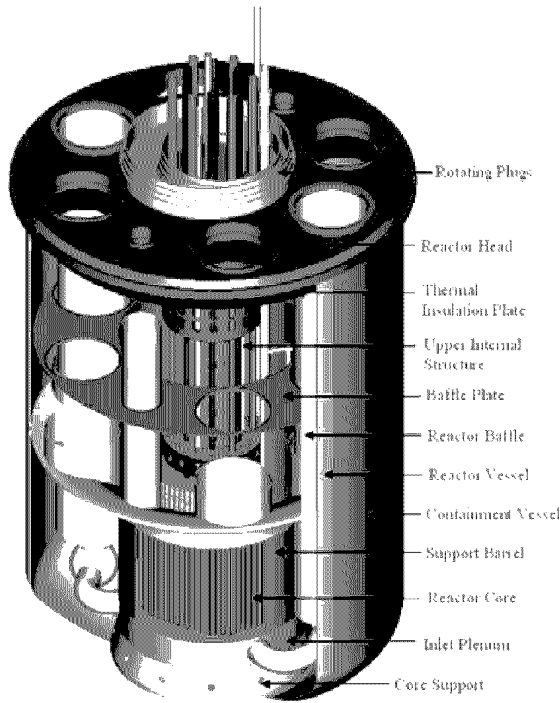
Fig. 1. Conceptually Designed KALIMER-600 Reactor Structures

Fig. 2. Crack-Initiation Evaluation Model

Fig. 3. Time-Dependent Loading History Diagram

2. CRACK-INITIATION EVALUATION MODEL

For this study, the crack-initiation evaluation model was a cylindrical structure with a welded Y-junction that simulated a discontinuous reactor internal structure. The material of the model was 316 stainless steel (SS), and the thickness, outer diameter, and height of the cylinder were 5 mm, 600 mm, and 500 mm, respectively. A through-wall defect that penetrated the wall was 20 mm in length and 0.25 mm in corner radius, and it was arranged in the circumferential direction at 230 mm from the upper surface of the model. Figure 2 shows the crack-initiation evaluation model.

The loading condition comprised a thermal loading and a mechanical loading, each having a cyclic history, as shown in Fig. 3. The mechanical loading was an axial tensile load, simulating the dead weight of the reactor structures. This axial tensile load was increased to 50 tons for a 1 minute startup, maintained for 64 minutes, and then removed. The temperature of the heating region of a specimen was increased from an initial temperature of 30°C to a maximum temperature of 545°C for 5 minutes, held at the maximum temperature for 1 hour, and then decreased to 30°C for 30 minutes. Both the mechanical loading and the thermal loading were repeatedly applied. This time-dependent thermal loading was performed to simulate the reactor startup-operation-shutdown process conservatively.
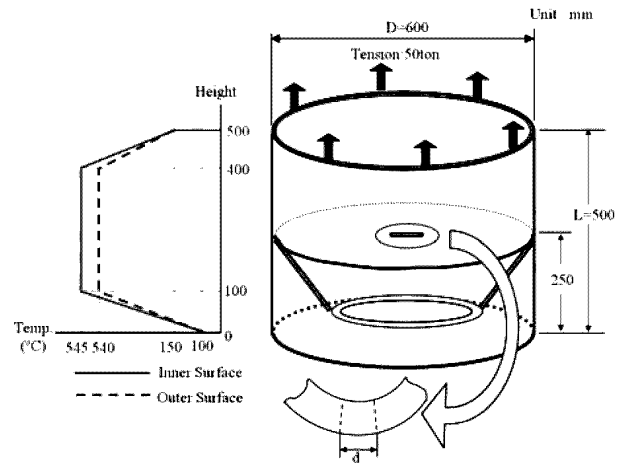
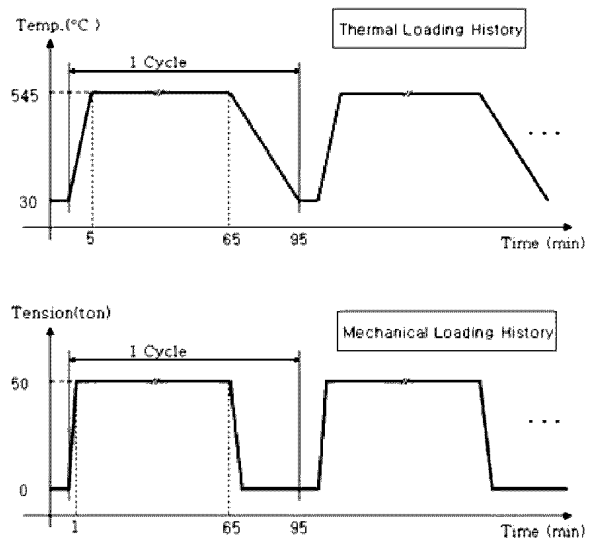The temperature difference between the inner surface and the outer surface of the model was approximated as 5°C, as shown in Fig. 2.

3. EVALUATION OF CRACK INITIATION

There are several kinds of crack-initiation evaluation methods, such as the time-dependent failure assessment diagram (TDFAD) method and the incubation time evaluation method of the UK code R5[5], as well as the σ_d method of the France code RCC-MR A16 guide. Consider-

ing the characteristics of each evaluation method, the crack initiation in this paper was evaluated by the σ_d method of the A16 guide due to its convenient applicability and the established material data. According to the A16 guide, a defect assessment for austenitic components is classified into one of two cases: a non-significant creep condition or a significant creep condition. In this study, a significant creep condition was applied because the normal operating temperature of the KALIMER-600 is 545°C.

3.1. Creep-Fatigue Interaction Diagram

Under a combined loading condition, the cyclic load generates structural fatigue damage, and creep damage is generated during a high-temperature (above 427°C) hold time. Therefore, the main factors inducing the crack initiation in the model of this study were fatigue and creep effects, as well as their interactions.

The creep-fatigue crack initiation is assessed based on the σ_d method [7]. The principle of this method is to determine the stress and the strain at a characteristic distance d from the crack tip, which follows from the material property. A characteristic distance for 316 SS in the A16 guide is d=0.05mm [4].

The evaluation method of the creep-fatigue crack initiation involves the fatigue usage fraction (A) and the creep usage fraction to a rupture (W). The fatigue crack initiation usage fraction is given by the ratio of the specified number of cycles n to the number of cycles prior to a fatigue initiation N_a, as shown in equation (1):

$$A_i = \frac{n_i}{N_{ai}} \qquad (1)$$

In equation (1), i refers to the cycle type, and N_a is the number of initiation cycles obtained from the RCC-MR A3 fatigue curve for a real strain range $\Delta \varepsilon_d$ at the distance d from the defect, allowing for a strain amplification due to plasticity and divided by the design safety factor k. For the current configuration of the model, $k = 1.5$, according to the A16 guide.

The creep crack initiation usage fraction is given by the ratio of the high temperature hold time t to the creep initiation time T obtained from the usual creep rupture properties S_r corresponding to the stress σ_d during the hold time at the distance d from the defect tip, as shown in equation (2).

$$W_i = \frac{t_i}{T_i} \qquad (2)$$

The total fatigue usage fraction and the total creep usage fraction are calculated on the basis of a linear sum

for all the specified cycles, as shown in equation (3).
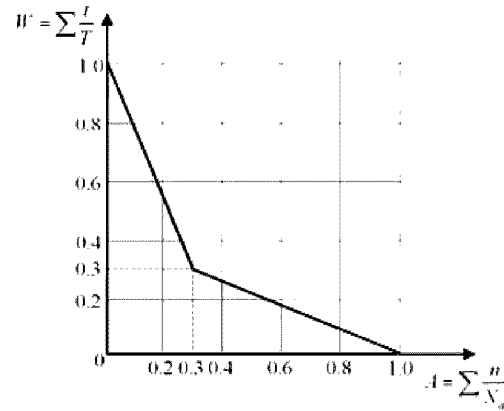
$$A = \Sigma A_i, \quad W = \Sigma W_i \qquad (3)$$

Fig. 4. Creep-Fatigue Interaction Diagram

The crack initiation is determined using the creep-fatigue interaction diagram, illustrated in Fig. 4. This creep-fatigue interaction diagram, which was generated based upon many tests and analyses results, was incorporated in the ASME code Section III, Subsection NH, as well as in the RCC-MR code, as cited in this paper. If the point of the co-ordinates (A, W) lies inside the creep-fatigue interaction diagram, the crack does not initiate within the period t under investigation. If (A, W) lies on and outside the curve, a creep-fatigue crack is initiated.

3.2. Calculation of the Fatigue Usage Fraction

To calculate the fatigue usage fraction for an evaluation model, the total real strain range, including the amplification of a strain due to plasticity, $(\Delta \varepsilon)_{el+pl}$ and creep, $\Delta \varepsilon_{cr}$, has to be obtained by adding the strain ranges, as expressed by equation (4).

$$\Delta \varepsilon = (\Delta \varepsilon)_{el+pl} + \Delta \varepsilon_{cr} \qquad (4)$$

In equation (4), the elastic-plus-plastic strain range, $(\Delta \varepsilon)_{el+pl}$, can be obtained by using the sum of the four strain components by considering the amplification due to plasticity, as shown in equation (5).

$$(\Delta \varepsilon)_{el+pl} = \Delta \varepsilon_1 + \Delta \varepsilon_2 + \Delta \varepsilon_3 + \Delta \varepsilon_4 \qquad (5)$$

In equation (5), the four strain components are as follows: $\Delta \varepsilon_1$ refers to the strain range from an elastic analysis; $\Delta \varepsilon_2$ refers to the plastic strain range due to a primary stress; $\Delta \varepsilon_3$ refers to the plastic strain range by applying Neuber's rule; and $\Delta \varepsilon_4$ refers to the plastic strain range due to triaxiality. The elastic strain range $\Delta \varepsilon_1$ can be obtained by equation (6).

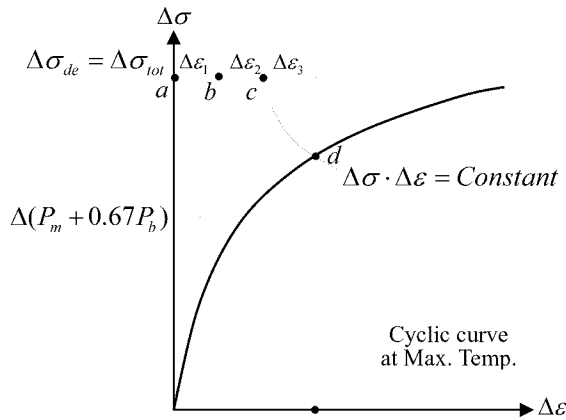$$\Delta \varepsilon_1 = \frac{2(1+v)}{3} \frac{\Delta \sigma_{de}}{E} \qquad (6)$$

In equation (6), $\Delta \sigma_{de}$ is the maximal elastic main stress range in the crack plane at distance d, v is the Poisson ratio, and E is the elastic modulus.

The value of $\Delta \varepsilon_2$ in equation (5) can be obtained from a primary stress range, as shown in Fig. 5. In the evaluation model, the primary membrane stress (P_m) is obtained from the axial tensile load, and the bending stress (P_b) is mainly obtained from the thermal stress caused by a temperature difference.

The value of $\Delta \varepsilon_3$ can be obtained from the path (c-d) of Fig. 5 by applying Neuber's rule, which the point (d) is the intersection point of the cyclic curve from the A3.59 in RCC-MR [3] and the hyperbola curve in equation (7).

$$\Delta \varepsilon \cdot \Delta \sigma = (\Delta \varepsilon_1 + \Delta \varepsilon_2) \cdot \Delta \sigma_{de} \qquad (7)$$

The value of $\Delta \varepsilon_4$ can be obtained by equation (8), as expressed below.

$$\Delta \varepsilon_4 = (K_v - 1.0)\Delta \varepsilon_1 \qquad (8)$$

In equation (8), K_v is the coefficient obtained for the value of $\Delta \sigma_{de}$ by using the curves and tables.

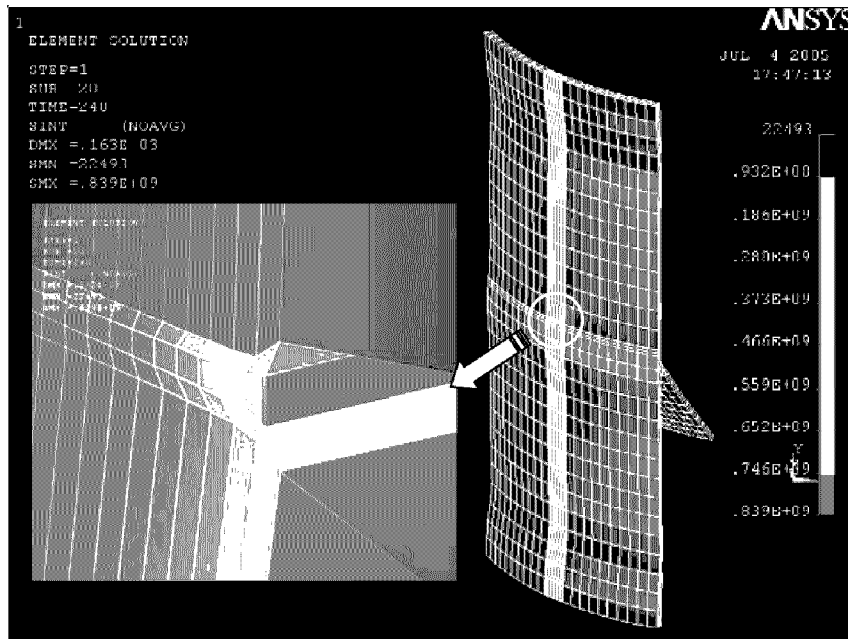To calculate the elastic stress range $\Delta \sigma_{de}$ in the evalua-

Fig. 5. Diagram of Determination of the Strain Range Components

Fig. 6. FE Analysis Stress Contour

Table 1. Material Properties of 316 Stainless Steel

Temperature (°C)	Elastic Modulus (GPa)	Poisson Ratio (-)	Density (kg/m³)	Thermal Expansion (1/°C)	Conductivity (J/s · m · °C)	Specific Heat (J/kg · °C)
20	195	0.27	7,946	15.1E-6	13.36	465.6
100	190	0.27	7,935	15.8E-6	14.70	494.7
200	184	0.28	7,890	16.5E-6	16.34	523.2
300	177	0.29	7,846	17.2E-6	17.94	544.3
400	168	0.29	7,892	17.8E-6	19.48	560.3
500	159	0.30	7,757	18.2E-6	20.96	573.1
600	149	0.31	7,713	18.6E-6	22.39	584.9

tion model, an FE analysis was carried out by using the ANSYS 9.0 software [8], as depicted in Fig. 6. The material properties of 316 SS at each temperature are shown in Table 1 [9]. In the FE analysis, a 1/4 axisymmetric modeling was applied. From the FE analysis results, $\Delta \sigma_{de}$ was determined to be 820 MPa at the crack front at the characteristic distance, and the strain range due to plasticity ($\Delta \varepsilon)_{el+pl}$ was 1.06 (%).

The creep strain $\Delta \sigma_{cr}$ should be obtained by adding the primary creep strain and the secondary creep strain. The primary creep strain is obtained by the following equation (9) from A3.59.

$$\varepsilon_f = C_1 \cdot t^{C_2} \cdot \sigma^{n_1} \qquad 425°C < T \le 700°C \qquad (9)$$

In equation (9), coefficients $C_1 = 1.6112 \times 10^{-11}$, $C_2 = 0.41741$ and $n_1 = 3.8632$ are the values from the function of the temperature given in Table A3.63 [3].

Equation (9) should be applied when the creep time is less than the end of the primary creep time, t_{fp} which can be obtained by equation (10).

$$t_{fp} = C_3 \cdot \sigma^{n_3} \qquad (10)$$

In equation (10), the coefficients ($C_3 = 3.1955 \times 10^{31}$ and $n_3 = -11.5869$) are the values from the function of the temperature given in Table A3.63.

Because the end of the primary creep time (t_{fp}) was estimated to be 314 hours for a cycle, a secondary creep strain was not considered in the evaluation model. From

equation (9), the creep strain $\Delta \varepsilon_{cr}$ was 0.076(%), and the real strain range $\Delta \varepsilon$ in equation (4) was 1.135(%). For the fatigue usage fraction, the real strain range was divided by 1.5, and the number of the initiation cycle N_a was determined from the fatigue curve A3.64 [3] corresponding to the real strain range. With this result, the fatigue usage fraction was determined by using equation (11).

$$A = \frac{n}{241} \qquad (11)$$

3.3. Calculation of the Creep Usage Fraction

The creep usage fraction in equation (2) is determined from the creep rupture time, and the creep rupture time is determined from the $\Delta \sigma_{kd}$ in equation (12), as follows.

$$\Delta \sigma_{kd} = \frac{\Delta \sigma^*}{2} \qquad (12)$$

In equation (12), $\Delta \sigma^*$ is the stress value determined from the S_r curve of A3.53 [3] corresponding to the strain range ($\Delta \varepsilon)_{el+pl}$.

The value of $\Delta \sigma_{kd}$ was estimated to be 319 MPa from equation (12) based upon the analysis result. The creep-rupture time T on the S_r curve corresponding to 545°C and $\Delta \sigma_{kd}$ is 125 hours. Therefore, the creep usage fraction is determined by equation (13), as follows.
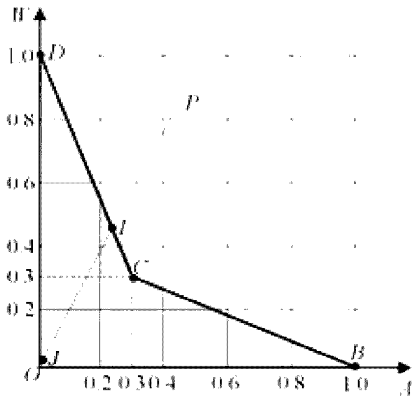
$$W = \frac{t}{125} \qquad (13)$$

Fig. 7. Evaluation Result of the Creep-Fatigue Crack Initiation

Fig. 8. Creep-Fatigue Test Facility

From equations (11) and (13), the evaluation point (A, W) is located along the path (O-P) in the creep-fatigue interaction diagram, as shown in Fig. 7. The point J is the initiation position for the 1st cycle. The crack is initiated at point I, where the path (O-P) intersects with the diagram curve (C-D). Therefore a creep-fatigue crack would initiate in 57 cycles and in 57 hours of a high-temperature hold time.

4. CRACK INITIATION TEST

To validate the applicability of the crack-initiation evaluation method for a cylindrical Y-junction structure of 316 SS containing a circumferential through-wall defect crack initiation, a creep-fatigue crack initiation test was carried out involving a cyclic axial tensile load with 1 hour of a hold time at a temperature of 545°C, as illustrated in Figs. 2 and 3.

4.1. Test Facilities

The creep-fatigue test facility was composed of a 1MN hydraulic actuator, a load frame and an anchored base plate, as shown in Fig. 8. The axial tensile load was applied using the hydraulic actuator, and the actuator control software used was the IST Labtronic 8800. The heating unit used to apply the thermal load was a high-frequency induction heater with 50 kHz and 50 kW capacities. This heater had 6 turns of copper coil surrounding the structural test model, and the induced current increased the temperature via resistance heating. Temperature control was accomplished by the PID control method, which was utilized to maintain a fixed temperature of 545°C for the test model. To achieve and control a fixed temperature for the test model, 24 channels of the K-type thermocouple were spot-welded onto the inner surface of the test model along the axial direction. Additionally, 10 channels were welded onto the outer surface in the axial direction, and 3 channels were welded
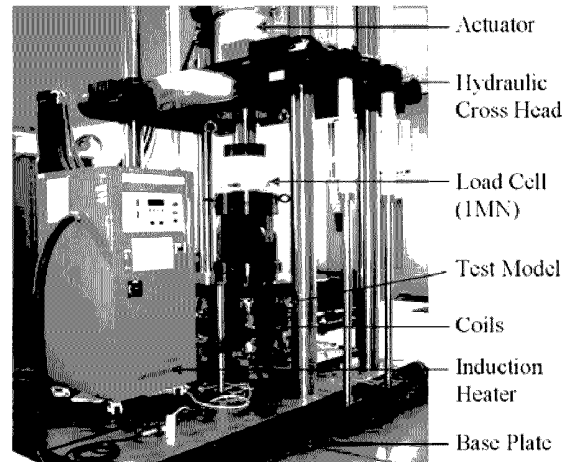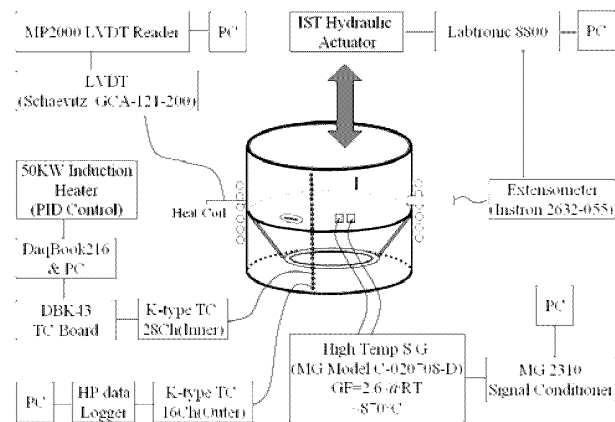

Fig. 9. Instrumentation and Control Arrangement

along the circumferential direction.

The IOTECH Daqbook 216 data acquisition board and the DBK19 thermocouple signal-conditioning card were connected to a PC system to collect the temperature data. Furthermore, the Agilent Tech Model 34970 data acquisition system was employed to measure the temperature and to increase the accuracy of the measurement, simultaneously [10]. The instrumentation and control arrangements are illustrated in Fig. 9.

4.2. Inspection and Results

A close inspection at the defect front is usually necessary to investigate the initiated crack length of a microscopic size. In our study, since a real-time inspection of the defect
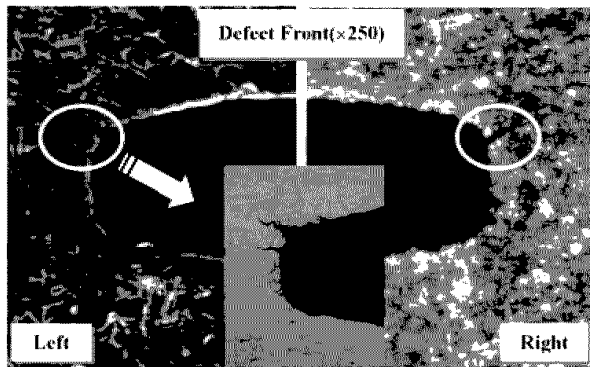
Fig. 10. Defect Front after 100th Cycle

front would have been difficult, due to the high-temperature conditions and the heating facility, the defect front was investigated with an optical microscope after the 100th cycle of the test. An optical microscope with the IMT i-Solution instrument, which can optically magnify up to 3500 times, was used for the crack front inspection. A surface inspection using the optical microscope was scheduled for every 100th cycle of testing to observe the crack initiation and growth, because a nondestructive inspection method was necessary for a continued testing of up to several hundreds of cycles. The crack initiation would occur along both the surface direction and the thickness direction. In this study, the surface crack initiation was observed and compared to the analysis results. The inspection and analysis of the crack growth along the thickness direction are to be reviewed in a subsequent paper.

The defect area on the test model was ground, polished and etched according to the procedure in reference [11]. Grinding was performed in four steps with Struers Sic-paper #120, #400, #800 and #1200, using a portable grinding tool. After the grinding, two steps of polishing were conducted using 6 μm polishing paper with 6 μm diamond paste and then 1 μm polishing paper with 1 μm diamond paste. The final step for the inspection was an etching, which was performed so that the defect front could be inspected with the optical microscope. Figure 10 shows the vicinity of the defect front after the 100th cycle magnified 250 times, which reveals the initiated crack.

5. CONCLUSIONS

In this study, an evaluation and test of a creep-fatigue crack initiation for a cylindrical Y-junction structure with a circumferential through wall defect were carried out. The creep-fatigue crack initiation was evaluated by using the creep-fatigue interaction diagram of the RCC-MR A16 guide, which is composed of a creep usage fraction and a

fatigue usage fraction. The evaluation result for the model shows that, under a combined mechanical loading and thermal loading, a creep-fatigue crack was initiated after about 57 cycles. An experimental test was performed for comparison with the evaluation result. After the 100th cycle, the defect front was investigated with an optical microscope, and a crack initiation was shown to have occurred. From the measured initiated crack length of 0.071 mm after the 100th cycle and by using 0.05 mm as the characteristic length of a crack initiation, we estimated that the observed crack initiation occurred after about the 70th test cycle, assuming linear microcrack growth. Though the crack may initiate in the circumferential direction and the radial direction, the crack initiation criteria are same for both directions. Therefore, the observation of the crack initiation in the only circumferential direction was performed in this study.

In this study, a structural test is in progress to inspect the crack growth behavior after initiation. Even though it is premature to draw a conclusion, the interim results show the conservatism of the analysis results following the σ_d approach for the crack initiation prediction. With further tests and analyses, which are planned for this study, the usefulness of the σ_d approach can be addressed confidently.

REFERENCES

[1] C.G. Park, J. B. Kim and J. H. Lee, "Fracture Mechanical Evaluation of High Temperature Structure and Creep-Fatigue Defect Assessment," KAERI/TR-2708/2004, Korea Atomic Energy Research Institute (2004).
[2] D. Hahn, et al., "Design Features of Advanced Sodium-Cooled Fast Reactor KALIMER-600," Proceedings of ICAPP '04, Pittsburgh, USA(2004).
[3] RCC-MR, design and construction rules for mechanical components of FBR nuclear islands, 2002 Edition, AFCEN (2002).
[4] A16 : Guide for Leak Before Break Analysis and Defect Assessment, 2002 Edition, AFCEN (2002).
[5] R5, Assessment Procedure for the High Temperature Response of Structures, BEGL(2003).
[6] D. Moulin, B. Drubay, L. Laiarinandrasana, "A synthesis of the fracture assessment methods proposed in the French RCC-MR code for high temperature," WRC Bulletin 440(1999).
[7] B. Drubay, S. Marie, S. Chapuliot, M.H. Lacire, B. Michel, H. Deschanels, "A16: Guide for Defect Assessment at Elevated Temperature," International Journal of Pressure Vessels and Piping, Vol.80, p.499-516 (2003).
[8] ANSYS user manual for version 9.0, Swanson Analysis System, Inc (2004).
[9] J. B. Kim, H. Y. Lee, C. G. Park, Y. S. Joo and J. H. Lee, "Cree-Fatigue Defect Assessment Test and Analysis of High Temperature Structure," KAERI/TR-2972/2005,

Korea Atomic Energy Research Institute (2005).

[10] J. B. Kim, H. Y. Lee, C. G.. Park, G. P. Jeon and J. H. Lee, "Creep-Fatigue Damage Evaluation of the 316SS Y-junction Structures n a Liquid Metal Reactor," *Proceedings of ICAPP '04*, Paper4323, Pittsburgh, PA USA (2004).

[11] J. S. Park, "Standard Procedure of Replication for High Temperature Equipment Life Estimation," *Proceedings of KSME*, **Vol.A**, No.24,9,pp.2381-2386 (2000).